jet INTL JOURNAL OF ELECTRONICS AND TELECOMMUNICATIONS, 2019, VOL. 65, NO. 1, PP. 103-109
Manuscript received August 6 2018; revised January, 2019. DOI: 10.24425/ijet.2019.126289

Full-duplex Cognitive Radio NOMA Networks: Outage and Throughput Performance Analysis

Thanh-Nam Tran, Dinh-Thuan Do, and Miroslav Voznak

***Abstract*—A novel non-orthogonal multiple access (NOMA) scheme is proposed to improve the throughput and the outage probability of the cognitive radio (CR) inspired system which has been implemented to adapt multiple services in the next-generation network (5G). In the proposed scheme, the primary source (PS) had sent a superposition code symbol with a predefined power allocation to relays, it decoded and forwarded (DF) a new superposition coded symbol to the destination with the other power allocation. By using a dual antenna at relays, it will be improved the bandwidth efficiency in such CR NOMA scheme. The performance of the system is evaluated based on the outage probability and the throughput with the assumption of the Rayleigh fading channels. According to the results obtained, it is shown that the outage probability and throughput of the proposed full-duplex (FD) in CR-NOMA with reasonable parameters can be able deploy in practical design as illustration in numerical results section.**

***Keywords*—Non-Orthogonal Multiple Access (NOMA), Cognitive Radio (CR), full-duplex (FD), outage probability, system throughput, achievabe bit rate**

I. INTRODUCTION

IN [1], the authors had shown that orthogonal frequency division multiple access (OFDMA) could be updated to the NOMA. As the future mobile network access technology, NOMA promises to become potential scheme for the next-generation (5G) network with higher requirement for system performance in term of throughput and bandwidth efficiency. In principle, using the superimposed signal at the transmitter and the continuous noise cancellation at the receiver, NOMA provides can detach signal [2], [3], and it is so-called as successive interference cancellation (SIC) to improve capacity. For downlink transmissions, by using different power factors, the source can transmit multiplexed signals for multiple destinations over the same subcarrier. The source detects the received signals at each destination. The first with the destination has the best signal to noise ratio (SNR) which is succeed through to the SIC. By using channel state information (CSI), the best quality signal regenerates by extract it from the received complex signal [4].

Regarding on recent advance in NOMA, the authors in [5] shown that with carefully chosen user rates and power coefficients for a single-input single-output (SISO) NOMA downlink system, NOMA can achieve superior ergodic sum rate and outage performance comparing to OMA. In [6], the capacity of cooperative relaying systems with NOMA is analyzed and by appropriate power allocation related to the sum rate performance advantage over cooperative relaying systems with OMA is also revealed. The authors in [7] further applies the NOMA principle to a multiple-input single-output (MISO) system and solves the downlink sum rate maximization problem. To consider a more practical situation, in [8] proposed full-duplex relay which decodes received symbols and simultaneously sends a superimposed composite signal to the destinations. To improve spectrum efficiency is the paradigm of underlay CR networks, which was proposed in [9] and has rekindled increasing interest in using the spectrum more efficiently. The key idea of underlay CR networks is that each secondary user (SU) allowed to access the spectrum of the primary users (PUs) if the SU meets a certain interference threshold in the primary network (PN). In [10], an underlay CR network considering the spatial distribution of the SU relays and PUs was considered, and its performance was evaluated by using stochastic geometry tools.

Motivated by above analysis, especially in [8] and [10], [11] we explore outage and throughput performance of potential CR-inspired NOMA scheme. The main contribution of this paper relies in idea of CR-NOMA opportunistically serve the primary user on the condition that the secondary users quality of service (QoS) is guaranteed.

More specifically, we perform CR NOMA with capability of energy harvesting [12-14] to evaluate outage and throughput performance. The main contributions of this paper can be summarized as

- We derived the closed-form expressions of outage and throughput performance
- The exactness of derived formula can be checked by matching Monte-Carlo simulation and analytical results.
- The impacts of transmit SNR at base station and the fixed rate can be contributed to system performance as in simulation results which help provide clear guideline for practical design in CR NOMA.

This study was presented in structure as follows. In section number II, Two schemes which are namely full-duplex and full-duplex with energy harvesting schemes were proposed, and we analysis on these schemes. In section number III, we have analyzed the system's performance using based on outage probability and system throughput. In section number IV, we proposed system parameters and presented numerical analysis results which were showed by figures by extracting from Matlab application exactly in truth. A conclusion of the results of our study was presented in section number V.

Thanh-Nam Tran and Miroslav Voznak are with Faculty of Electrical Engineering and Computer Science, Technical University of Ostrava, 17. listopadu 2172/15, 708 33 Ostrava-Poruba, Czech Republic (e-mail: thanh.nam.tran.st@vsb.cz, and miroslav.voznak@vsb.cz).

Dinh-Thuan Do is with Industrial University of Ho Chi Minh City, 12 Nguyen Van Bao, Ho Chi Minh City, Vietnam. (e-mail: dodinhthuan@iuh.edu.vn).

II. System Models

In this study, a wireless downlink system consists of a transmitter and receivers in that if there has any receiver with a weak signal, the receiver with a better signal is selected as the relay. We assumed that each relay was equipped with a DA and operated in full-duplex mode. To brief the formula expressed in the next section, Primary Source, Primary Relay (PR), Secondary Relay (SR), Primary Destination (PD) and Secondary Destination (SD) were denoted by PS, PR, SR, PD and SD in the formulas below, respectively. Another assumption, the channels between the PS transmit to PR and SR are two independent random variables following a complex Gaussian distribution with zero mean and variances, i.e., $h_{PS,PR} \sim CN\left(0, \sigma^2_{PS,PR}\right)$ and $h_{PS,SR} \sim CN\left(0, \sigma^2_{PS,SR}\right)$. The advantage of NOMA is that any receiver with a good signal can be selected to become a transmitter for transmitting the signal to a receiver with poor signal quality. In particularly, if the signal channels from PS to PD and SD are poor. In this case, two other receiver devices which have strong signal quality, are used as relays for dual-hop cooperative transmission. P_{PS}, P_{PR}, P_{SR} were denoted the transmission power of the PS, PR and SR, respectively. An assumption is allowed in NOMA, the signal transmission channels from PS to relays are $|h_{S,PR}|^2$ and $|h_{S,SR}|^2$, where $|h_{S,PR}|^2 > |h_{S,SR}|^2$ is required. In additional, we assumed that signal transmission channels in paired PR, PD and paired SR, SD and did not interfere with each other as Fig. 1.

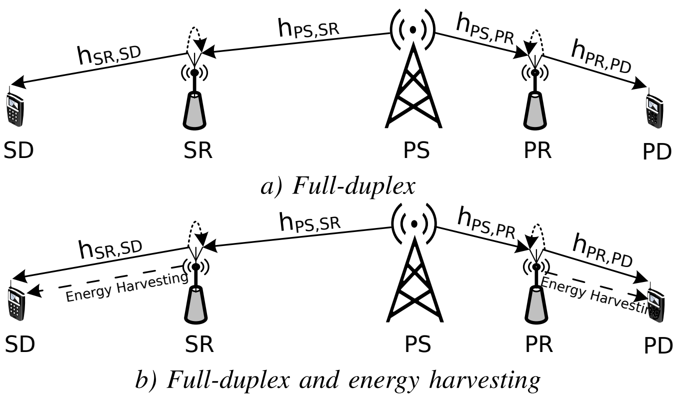

Fig. 1. CR-NOMA scheme

For bandwidth efficiency enhancement, fig. 1a is a proposed model which is an illustration of FD in CR-NOMA. For completed a transmission round, it need have two time slots to transmit signals from PS to PD, and PS to SD. In the first time slot (FTS), PS sent a mixed signal $S^{FD}_{PS} = \left(\sqrt{\alpha_{PS} P_{PS}} m_1 + \sqrt{\beta_{PS} P_{PS}} m_2\right)$, where m_1 and m_2 are the incoming signals for PD and SD, respectively. α_{PS} and β_{PS} were denoted as power factors, where $\alpha_{PS} + \beta_{PS} = 1$, and P_{PS} is a transmit power of PS.

At PR, the received signals were as following expression

$$y^{FD}_{PS,PR} = h_{PS,PR}\left(\sqrt{\alpha_{PS} P_{PS}} m_1 + \sqrt{\beta_{PS} P_{PS}} m_2\right) + h_{LI,PR}\sqrt{\omega_{PR} P_{PR}} i_{LI,PR} + n_{PR}. \quad (1)$$

Similarly, considering on SR, the received signals is expressed

$$y^{FD}_{PS,SR} = h_{PS,SR}\left(\sqrt{\alpha_{PS} P_{PS}} m_1 + \sqrt{\beta_{PS} P_{PS}} m_2\right) + h_{LI,SR}\sqrt{\omega_{SR} P_{SR}} i_{LI,SR} + n_{SR}, \quad (2)$$

where n_{PR} and n_{SR} are additive white Gaussian noise (AWGN) and following $n_{PR} = n_{\mathrm{SR}} \sim CN(0, N_0)$, and the residual loop self-interference (LI) is modeled as a Rayleigh fading feedback channel with coefficient $h_{LI,PR} = h_{LI,SR}$. The received signals will be decoded by using SIC at both relay. At PR, m_2 symbol will be first decoded by treating m_1 as interference and it has the achievable signal-to- interference-plus-noise ratio (SINR) as

$$\gamma^{FD}_{PR\to m_2} = \frac{|h_{PS,PR}|^2 \beta_{PS} P_{PS}}{|h_{PS,PR}|^2 \alpha_{PS} P_{PS} + |h_{LI,PR}|^2 \omega_{PR} P_{PR} + N_0} = \frac{|h_{PS,PR}|^2 \beta_{PS} \rho_{PS}}{|h_{PS,PR}|^2 \alpha_{PS} \rho_{PS} + |h_{LI,PR}|^2 \omega_{PR} \rho_{PR} + 1}, \quad (3)$$

where $\rho_{PS} = \frac{P_{PS}}{N_0}$, $\rho_{PR} = \frac{P_{PR}}{N_0}$ and ω_{PR} is the switching operation factor. We assumed that PR was operated in full-duplex mode and hence we have $\omega_{PR} = 1$.

In phase 2, after decoding m_2, m_2 would be subtracted from the mixed signal with AWGN and the loop interference (LI). Therefore, it has the achievable SINR as

$$\gamma^{FD}_{PR\to m_1} = \frac{|h_{PS,PR}|^2 \alpha_{PS} \rho_{PS}}{|h_{LI,PR}|^2 \omega_{PR} \rho_{PR} + 1} \quad (4)$$

In the same method, at SR, m_2 was decoded by treating m_1 as interference in phase 1 and it has the achievable SINR as

$$\gamma^{FD}_{PR\to m_2} = \frac{|h_{PS,SR}|^2 \beta_{PS} \rho_{PS}}{|h_{PS,PR}|^2 \alpha_{PS} \rho_{PS} + |h_{LI,SR}|^2 \omega_{SR} \rho_{SR} + 1}, \quad (5)$$

where $\rho_{SR} = \frac{P_{SR}}{N_0}$, and in phase 2, it subtracted m_2 from the signals

$$\gamma^{FD}_{SR\to m_1} = \frac{|h_{PS,SR}|^2 \alpha_{PS} \rho_{PS}}{|h_{LI,SR}|^2 \omega_{SR} \rho_{SR} + 1}. \quad (6)$$

Then, the achievable rates at both relay are

$$R^{FD}_{\mathrm{PR}\to \mathrm{m}_i} = \frac{1}{2}\log_2\left(1 + \gamma^{FD}_{\mathrm{PR}\to \mathrm{m}_i}\right), \quad (7)$$

and

$$R^{FD}_{\mathrm{SR}\to \mathrm{m}_i} = \frac{1}{2}\log_2\left(1 + \gamma^{FD}_{\mathrm{SR}\to \mathrm{m}_i}\right), \quad (8)$$

where $i = \{1, 2\}$.

In second time slot (STS), $\bar{m}_1$ symbols was been sent to PD by PR, while $\bar{m}_2$ was been sending to SD by SR in paired. PD and SD would receive the signals which were presented, respectively, as

$$y^{FD}_{PD} = h_{PR,PD}\sqrt{\varepsilon_{PR} P_{PR}}\bar{m}_1 + N_0, \quad (9)$$

and

$$y^{FD}_{\mathrm{SD}} = h_{SR,SD}\sqrt{\varepsilon_{SR} P_{SR}}\bar{m}_2 + N_0. \quad (10)$$

Thus, SINRs could be written for PD and SD, respectively, as

$$\gamma_{PD}^{FD} = \frac{|h_{PR,PD}|^2 \varepsilon_{PR} P_{PR}}{N_0} = |h_{PR,PD}|^2 \varepsilon_{PR} \rho_{PR}, \tag{11}$$

and

$$\gamma_{SD}^{FD} = \frac{|h_{SR,SD}|^2 \varepsilon_{SR} P_{SR}}{N_0} = |h_{SR,SD}|^2 \varepsilon_{SR} \rho_{SR}. \tag{12}$$

Next, we consider PD and SD on the achievable rates as following expressed

$$R_{PD}^{FD} = \frac{1}{2}\log_2\left(1+\gamma_{\mathrm{PD}}^{FD}\right), \tag{13}$$

and

$$R_{\mathrm{SD}}^{FD} = \frac{1}{2}\log_2\left(1+\gamma_{SD}^{FD}\right). \tag{14}$$

III. Performance Analysis

A. Outage Probability

We predefined value of minimum rates which were denoted by R_1^{th} and R_2^{th} for PD and SD, respectively. If the achievable rates is less than the minimum rates, an outage event will be occurred then.

Proposition 1: In such CR NOMA, we define $P_{O,PD}^{\mathrm{FD}}$ is the outage probability at PD

$$\begin{aligned} P_{O,PD}^{FD} &= 1 - P_{PD}^{FD} \\ &= 1 - \Pr\left(\min\left\{R_{PR\to m_1}^{FD}, R_{PD}^{FD}\right\} > R_1^{th} \; and \right. \\ &\left. \min\left\{R_{PR\to m_2}^{FD}, R_{SR\to m_2}^{FD}\right\} > R_2^{th}\right) \\ &= 1 - \left(\min\left\{\tau_1, \tau_3\right\}\right)(\tau_2)(\tau_4), \end{aligned} \tag{15}$$

and the outage probability at SD is expressed as $P_{O,SD}^{FD}$

$$\begin{aligned} P_{O,SD}^{FD} &= 1 - P_{SD}^{FD} \\ &= 1 - \Pr\left(R_{PR\to m_1}^{FD} > R_1^{th} \; and \right. \\ &\left. \min\left\{R_{PR\to m_2}^{FD}, R_{SR\to m_2}^{FD}, R_{SD}^{FD}\right\} > R_2^{th}\right) \\ &= 1 - \left(\min\left\{\tau_1, \tau_3\right\}\right)(\tau_4)(\tau_5), \end{aligned} \tag{16}$$

where τ_1, τ_2, τ_3, τ_4, and τ_5 are given by (17), (18), (19), (20), and (21), respectively,

$$\tau_1 = e^{-\left(\frac{\chi_1}{\psi_1}\right)} \frac{\psi_1}{\psi_1 + \chi_1 \omega_{PR} \rho_{PR} \sigma_{h_{LI,PR}}^2}, \tag{17}$$

$$\tau_2 = e^{-\left(\frac{\chi_1}{\rho_{PR}\sigma_{h_{PR,PD}}^2}\right)}, \tag{18}$$

$$\tau_3 = e^{-\left(\frac{\chi_2}{\psi_3}\right)} \frac{\psi_3}{\psi_3 + \chi_2 \omega_{PR} \rho_{PR} \sigma_{h_{LI,PR}}^2}, \tag{19}$$

$$\tau_4 = e^{-\left(\frac{\chi_2}{\psi_4}\right)} \frac{\psi_4}{\psi_4 + \chi_2 \omega_{SR} \rho_{SR} \sigma_{h_{LI,SR}}^2}, \tag{20}$$

$$\tau_5 = e^{-\left(\frac{\chi_2}{\rho_{SR}\sigma_{h_{SR,SD}}^2}\right)}. \tag{21}$$

B. System Throughput

In this section, we analyzed the throughput of the proposed scheme. We denoted P_{Thr}^{DA} as the throughput of the proposed scheme. The throughput performance of CR-NOMA using FD scheme at the fixed rare R_1^{th}, R_2^{th} and it can be expressed as

$$P_{Thr}^{FD} = \left(1 - P_{O,PD}^{FD}\right) R_1^{th} + \left(1 - P_{O,SD}^{FD}\right) R_2^{th}. \tag{22}$$

C. The proposed power reallocation at Relays

As illustration in Fig. 1b, we propose different power factors which were called ε_{PR} and ε_{SR} for PR and SR, respectively. Instead of using 100% of the transmit power, excess power is used to transmit the energy to the receiver. In such case, the destination users, i.e. SD and PD are assigned as energy harvesting-enabled equipment. Therefore, the signals received at PR and SR are expressed respectively as

$$\begin{aligned} y_{PD}^{FD,EH} &= h_{PR,PD}\left(\sqrt{\varepsilon_{PR} P_{PR}}\bar{m}_1 \right. \\ &\left. + \sqrt{\left(1-\varepsilon_{PR}\right) P_{PR}}\phi\right) + N_0, \end{aligned} \tag{23}$$

and

$$\begin{aligned} y_{\mathrm{SD}}^{FD,EH} &= h_{SR,SD}\left(\sqrt{\varepsilon_{SR} P_{SR}}\bar{m}_2 \right. \\ &\left. + \sqrt{\left(1-\varepsilon_{SR}\right) P_{SR}}\phi\right) + N_0, \end{aligned} \tag{24}$$

where $\varepsilon_{PR} = \alpha_{\mathrm{PS}}$, $\varepsilon_{SR} = \beta_{\mathrm{PS}}$, and ϕ is a silent signal which is intended for wireless power transfer.

At PD, the received signal which was decoded by extract N_0 and then we computed SINR as

$$\gamma_{PD}^{FD,EH} = \frac{|h_{PR,PD}|^2 \varepsilon_{PR} P_{PR}}{N_0} = |h_{PR,PD}|^2 \varepsilon_{PR} \rho_{PR}, \tag{25}$$

and SINR of SD was computed as

$$\gamma_{\mathrm{SD}}^{FD,EH} = \frac{|h_{SR,SD}|^2 \varepsilon_{SR} P_{SR}}{N_0} = |h_{SR,SD}|^2 \varepsilon_{SR} \rho_{SR}. \tag{26}$$

Similarly (13) and (14), (25) and (26) can be obtained the achievable rates at PD and SD as

$$R_{\mathrm{PD}}^{\mathrm{FD},EH} = \frac{1}{2}\log_2\left(1 + |h_{PR,PD}|^2 \varepsilon_{PR} \rho_{PR}\right), \tag{27}$$

and

$$R_{SD}^{FD,EH} = \frac{1}{2}\log_2\left(1 + |h_{SR,SD}|^2 \varepsilon_{SR} \rho_{SR}\right). \tag{28}$$

In second case where the destination users can be harvested energy from the relay, we can perform the detail evaluation as below

Proposition 2: Similarly (15) and (16), $P_{O,PD}^{FD,EH}$ and $P_{O,SD}^{FD,EH}$ are denoted as the outage probability at PD and SD, respectively, which can be expressed by

$$P_{O,PD}^{FD} = 1 - P_{PD}^{FD} = 1 - \Pr\left(\min\left\{R_{PR\to m_1}^{FD}, R_{PD}^{FD,EH}\right\} > R_1^{th} \text{ and } \min\left\{R_{PR\to m_2}^{FD}, R_{SR\to m_2}^{FD}\right\} > R_2^{th}\right), \tag{29}$$

and

$$P_{O,SD}^{FD} = 1 - P_{SD}^{FD} = 1 - \Pr\left(R_{PR\to m_1}^{FD} > R_1^{th} \text{ and } \min\left\{R_{PR\to m_2}^{FD}, R_{SR\to m_2}^{FD}, R_{SD}^{FD,EH}\right\} > R_2^{th}\right). \tag{30}$$

Thus, the system throughput, namely $P_{Thr}^{FD,EH}$, is computed as expression

$$P_{Thr}^{FD,EH} = \left(1 - P_{O,PD}^{FD,EH}\right) R_1^{th} + \left(1 - P_{O,SD}^{FD,EH}\right) R_2^{th}. \tag{31}$$

IV. Numerical Results

In this section, we perform analysis and simulation the proposed model. Firstly, it can be provided valuable evaluations and simulations regarding on the outage probability of this model, which demonstrates the quality of the system. It can be determined that the system with the lower outage probability, it means that the system has good signal transmission performance. The results and a few important parameters of the system are presented below.

Fig. 2 illustrates the outage probability achieved by our proposed system model with $\alpha_S = 0.2$, $\beta_S = 0.8$, $R_1^{th} = R_2^{th} = \{0.2, 0.5, 0.7\}$ $bits/second/Hz$, channel gains is set as $|h_{PS,PR}|^2 = \sigma_{PS,PR}^2 = 5$, $|h_{PS,SR}|^2 = \sigma_{PS,SR}^2 = 1$, $|h_{PR,PD}|^2 = \sigma_{PR,PD}^2 = 1$, $|h_{SR,SD}|^2 = \sigma_{SR,SD}^2 = 1$, $|h_{LI,PR}|^2 = \sigma_{LI,PR}^2 = |h_{LI,SR}|^2 = \sigma_{LI,SR}^2 = 0.05$ and the transmission SNR of the PS from 0 dB to 50 dB to compare the outage probability of various bit rates. As can be seen from the Fig. 2, with $R_1^{th} = R_2^{th} = 0.2$, the results of the outage probability are the best performance and worse when increased bit rates. With the increasing level of transmit SNR, the outage performance of these cases will be enhanced and hardly improves even at high SNR. Such phenomenon can be explained by the fact that the outage performance very much relies on the power for signal processing. The performance gap of two schemes will be clearer at very high value of transmit SNR.

Due to the role of target rate on outage performance, each scheme achieved the different performance and such performance gap changes linear as varying the transmit SNR at the source, which are shown in Fig. 2. It is seen that higher target rate leads to worse outage performance.

In Fig. 3, it displays the results of systhem throughput as comparion with different the target rate in proposed scheme, but at high transmit SNR, such throughput remains the floor value.

Fig. 4 depicts the outage probabilities for each user in the considered CR-NOMA, where $\varepsilon_{PR} = \alpha_{PS} = 0.2$, $\varepsilon_{PR} = \beta_{PS} = 0.8$ and the SNR threshold for $R_1^{th} = R_2^{th} = \{0.2, 0.5, 0.7\}$ $(b/s/Hz)$. That means at PR uses only 20% of power to send signals to PD, the remaining power is used to transmit energy. Similarly, SR uses 80% of power to send signals to SD, the remaining power is used to transmit energy, too. The results show that the proposed energy harvesting for the user PD and SD in such NOMA scheme can dramatically improve the outage performance with higher power allocation. In case of more power allocated for the NOMA energy harvested user, the outage performance of NOMA is also gradually decreased. The results also show that the performance curve for simulation and analytical in each scheme is almost matched very well.

Similarly, Fig. 5 compare throughput applying energy harvesting for PD, SD. In generally, it can still achieve the similar throughput performance as the case, in which energy harvesting supply enough energy for signal processing at destination users. In SNR range from 0 dB to 15 dB, the system throughput with $R_1^{th} = R_2^{th} = 0.2$ has the best quality.

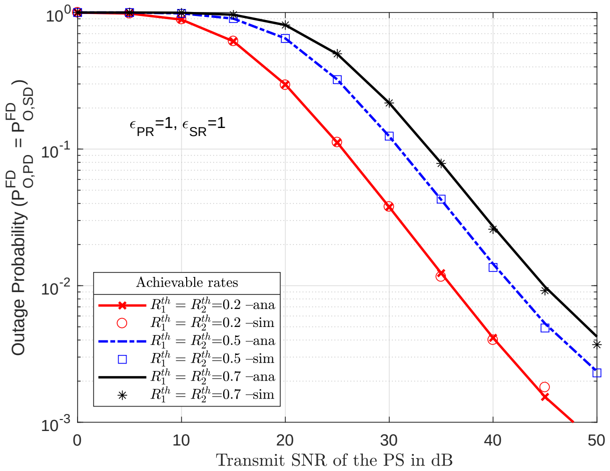

Fig. 2. The outage probability of CR-NOMA using FD scheme on $R_1^{th} = R_2^{th} = \{0.2, 0.5, 0.7\}$

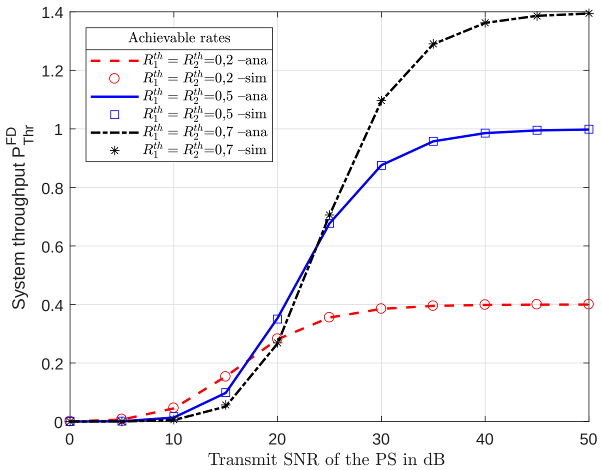

Fig. 3. The throughput of CR-NOMA using FD on different target rates $R_1^{th} = R_2^{th} = \{0.2, 0.5, 0.7\}$

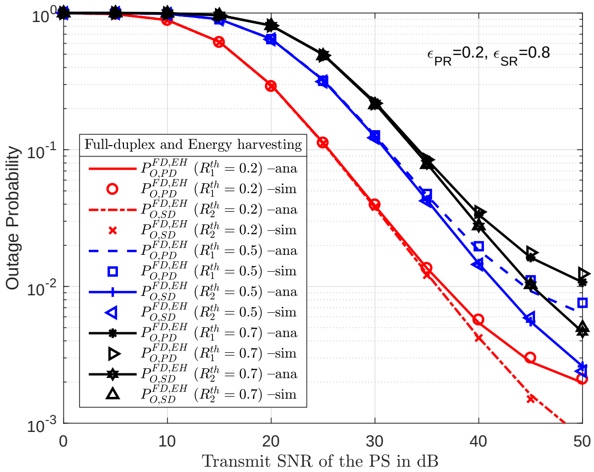

Fig. 4. The outage probability of CR-NOMA scheme on $(\varepsilon_{PR} = \alpha_{PS} = 0.2, \varepsilon_{SR} = \beta_{PS} = 0.8)$

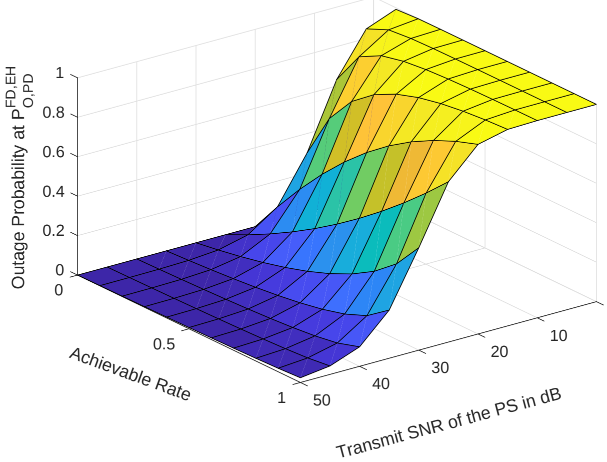

Fig. 6. The outage probability at PD on $R_1^{th} = R_2^{th} = \{0 : 1\}$

By increasing SNR over 15 dB, the system throughput is affected by the fixed rate.

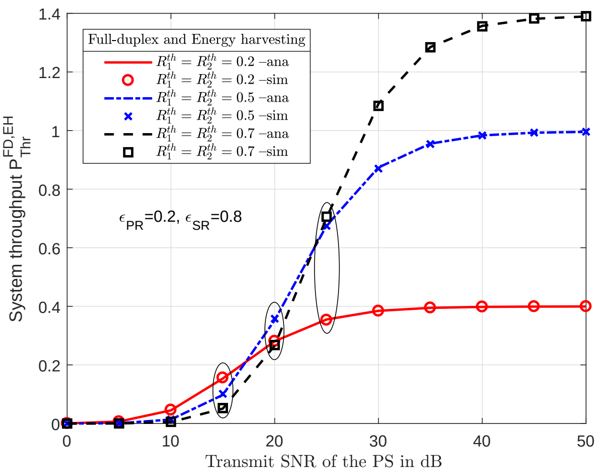

Fig. 5. The system throughput of CR-NOMA

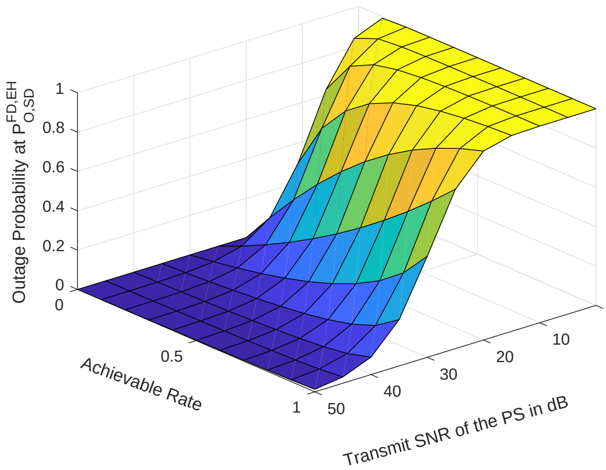

Fig. 7. The outage probability at SD on $R_1^{th} = R_2^{th} = \{0 : 1\}$

Fig. 6 and fig. 7 depict the result analysis of PD, SD as varying the fixed rate and SNR at the base station, i.e. $R_1^{th} = R_2^{th} = \{0 : 1\}$ and SNR from 0 to 50 dB.

In final experiment, Fig. 8 illustrate the results of system throughput on $R_1^{th} = R_2^{th} = \{0 : 1\}$ and SNR from 0 to 50 dB. The system throughput is highest where SNR in 50 dB and the fixed rate in 1 bps.

V. Conclusion

In this article, our study analyzed the outage and throughput performance based on CR-NOMA scheme over Rayleigh fading channels. We have solved the exact expressions of the outage probability for both full-duplex and full-duplex with energy harvesting schemes. The results of our study presented in Numerical Results section are reliable because they are accurately analyzed and simulated by the Matlab application. Finally, the FD and EH models that we have proposed can be applied in new generation networks.

Appendix

Proof of Proposition 1

First, the probability density function (PDF) of Rayleigh fading channels is presented as

$$f_{|h|^2}(x) = \frac{1}{\sigma_h^2} e^{-\frac{x}{\sigma_h^2}}, \quad (32)$$

where $\sigma_h^2 = E\left[|h|^2\right]$.

By applying (32), We can compute the outage probability for PD which is denoted by $P_{O,PD}^{FD}$ as below

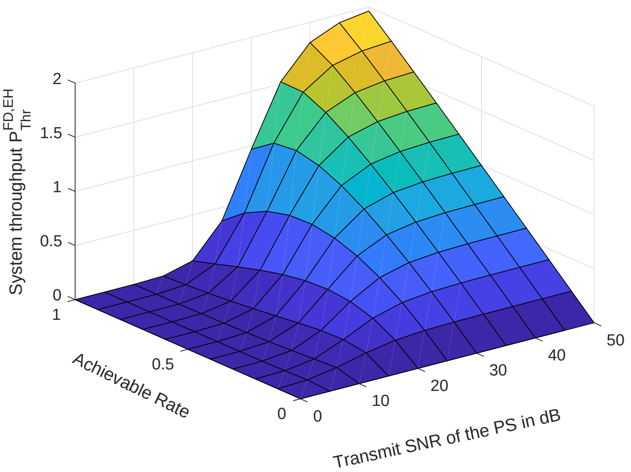

Fig. 8. System throughput on $R_1^{th} = R_2^{th} = \{0:1\}$

$$\begin{aligned}
&P_{O,PD}^{FD}\\
&= 1 - P_{PD}^{FD}\\
&= 1 - \Pr\left(\min\left\{R_{PR\to m_1}^{FD}, R_{PD}^{FD}\right\} > R_1^{th} \text{ and }\right.\\
&\left.\min\left\{R_{PR\to m_2}^{FD}, R_{SR\to m_2}^{FD}\right\} > R_1^{th}\right)\\
&= 1 - \Pr\left(\min\left(\underbrace{|h_{PS,PR}|^2 \geq \frac{\chi_1\left(|h_{LI,PR}|^2\omega_{PR}\rho_{PR}+1\right)}{\alpha_{PS}\rho_{PS}}}_{\tau_1},\right.\right.\\
&\left.\left.\underbrace{|h_{PS,PR}|^2 \geq \frac{\chi_2\left(|h_{LI,PR}|^2\omega_{PR}\rho_{PR}+1\right)}{\left(\beta_{PS}-\chi_2\alpha_{PS}\right)\rho_{PS}}}_{\tau_3}\right)\right)\\
&\Pr\left(\underbrace{|h_{PR,PD}|^2 \geq \frac{\chi_1}{\varepsilon_{\mathrm{PR}}\rho_{PR}}}_{\tau_2}\right)\\
&\Pr\left(\underbrace{|h_{PS,SR}|^2 \geq \frac{\chi_2\left(|h_{LI,SR}|^2\omega_{SR}\rho_{SR}+1\right)}{\left(\beta_{PS}-\chi_2\alpha_{PS}\right)\rho_{PS}}}_{\tau_4}\right)\\
&= 1 - \left(\min\left\{\tau_1,\tau_3\right\}\right)\left(\tau_2\right)\left(\tau_4\right),
\end{aligned} \tag{33}$$

where $|h_{PS,PR}|^2$, $|h_{PS,SR}|^2$, $|h_{LI,PR}|^2$, $|h_{LI,SR}|^2$, and $|h_{PR,PD}|^2$ are independent random variables with Rayleigh distribution.

Following several computation steps as below, τ_1, τ_2, τ_3, τ_4, and τ_5 can be proved by (34), (35), (36), (37), and (38) completely

$$\begin{aligned}
\tau_1 &= \Pr\left\{|h_{PS,PR}|^2 \geq \frac{\chi_1\left(|h_{LI,PR}|^2\omega_{PR}\rho_{PR}+1\right)}{\alpha_{PS}\rho_{PS}}\right\}\\
&= \int_0^{+\infty}\int_{\frac{\chi_1(\omega_{PR}\rho_{PR}y+1)}{\alpha_{PS}\rho_{PS}}}^{+\infty} f_{|h_{PS,PR}|^2}(x)\, f_{|h_{LI,PR}|^2}(y)dxdy\\
&= e^{-\left(\frac{\chi_1}{\psi_1}\right)}\frac{\psi_1}{\psi_1+\chi_1\omega_{PR}\rho_{PR}\sigma_{h_{LI,PR}}^2},
\end{aligned} \tag{34}$$

where $\psi_1 = \alpha_{PS}\rho_{PS}\sigma_{h_{PS,PR}}^2$ and $\chi_1 = 2^{2R_1^{th}} - 1$.

$$\begin{aligned}
\tau_2 &= \Pr\left\{|h_{PR,PD}|^2 \geq \frac{\chi_1}{\varepsilon_{\mathrm{PR}}\rho_{PR}}\right\}\\
&= e^{-\left(\frac{\chi_1}{\varepsilon_{\mathrm{PR}}\rho_{PR}\sigma_{h_{PR,PD}}^2}\right)}.
\end{aligned} \tag{35}$$

Similarly, we can obtain

$$\begin{aligned}
\tau_3 &= \Pr\left\{|h_{PS,PR}|^2 \geq \frac{\chi_2\left(|h_{LI,PR}|^2\omega_{PR}\rho_{PR}+1\right)}{\left(\beta_{PS}-\chi_2\alpha_{PS}\right)\rho_{PS}}\right\}\\
&= e^{-\left(\frac{\chi_2}{\psi_3}\right)}\frac{\psi_3}{\psi_3+\chi_2\omega_{PR}\rho_{PR}\sigma_{h_{LI,PR}}^2},
\end{aligned} \tag{36}$$

where $\psi_3 = \left(\beta_{PS}-\chi_2\alpha_{PS}\right)\rho_{PS}\sigma_{h_{PS,PR}}^2$ and $\chi_2 = 2^{2R_1^{th}} - 1$. Next, we continue compute

$$\begin{aligned}
\tau_4 &= \Pr\left\{|h_{PS,SR}|^2 \geq \frac{\chi_2\left(|h_{LI,SR}|^2\omega_{SR}\rho_{SR}+1\right)}{\left(\beta_{PS}-\chi_2\alpha_{PS}\right)\rho_{PS}}\right\}\\
&= e^{-\left(\frac{\chi_2}{\psi_4}\right)}\frac{\psi_4}{\psi_4+\chi_2\omega_{SR}\rho_{SR}\sigma_{h_{LI,PR}}^2},
\end{aligned} \tag{37}$$

where $\psi_4 = \left(\beta_{PS}-\chi_2\alpha_{PS}\right)\rho_{PS}\sigma_{h_{PS,SR}}^2$.

$$\begin{aligned}
\tau_5 &= \Pr\left\{|h_{SR,SD}|^2 \geq \frac{\chi_2}{\varepsilon_{\mathrm{SR}}\rho_{SR}}\right\}\\
&= e^{-\left(\frac{\chi_2}{\varepsilon_{\mathrm{SR}}\rho_{SR}\sigma_{h_{SR,SD}}^2}\right)}.
\end{aligned} \tag{38}$$

Similarly, we can compute outage probability for SD which is denoted by $P_{O,SD}^{FD}$ as below

$$\begin{aligned}
P_{O,SD}^{FD} &= 1 - P_{SD}^{FD}\\
&= 1 - \Pr\left(R_{PR\to m_1}^{FD} > R_1^{th} \text{ and }\right.\\
&\left.\min\left\{R_{PR\to m_2}^{FD}, R_{SR\to m_2}^{FD}, R_{SD}^{FD}\right\} > R_2^{th}\right)\\
&= 1 - \left(\min\left\{\tau_1,\tau_3\right\}\right)\left(\tau_4\right)\left(\tau_5\right).
\end{aligned} \tag{39}$$

Proof of Proposition 2

For energy harvesting, (35) can be rewritten by

$$\tau_2 \triangleq e^{-\left(\frac{x_1}{\varepsilon_{PR}\rho_{PR}\sigma^2_{h_{PR,PD}}}\right)}, \tag{40}$$

where $\varepsilon_{PR} = \omega_{PR} = 1$ if PR uses 100% transmit power or $\varepsilon_{PR} \triangleq \Delta_{PR} \triangleq \alpha_P S$ if it does not use 100% transmit power.

Similarly, we can rewritten (38) as

$$\tau_5 \triangleq e^{-\left(\frac{x_2}{\varepsilon_{SR}\rho_{SR}\sigma^2_{h_{SR,SD}}}\right)}, \tag{41}$$

where $\varepsilon_{SR} \triangleq \Delta_{SR} \triangleq \beta_{PS}$ if SR does not use 100% transmit power.

End of proof.

REFERENCES

[1] H. Zhu, and J. Wang, Chunk-based resource allocation in OFDMA systemsPart I: Chunk allocation, *IEEE Trans. Commun.*, vol. 57, no. 9, pp. 27342744, Sep. 2009.

[2] A. Benjebbour et al, Concept and practical considerations of non-orthogonal multiple access (NOMA) for future radio access. in Proc, *Int. Symp. Intell. Signal Process. Commun. Syst. (ISPACS)*, Naha, Japan, Nov. 2013. pp. 770774.

[3] D. Tse, and P. Viswanath, Fundamentals of Wireless Communication, Cambridge, U.K.: Cambridge Univ. Press, 2005.

[4] R. Zhang, and L. Hanzo, A unified treatment of superposition coding aided communications: Theory and practice, *IEEE Commun. Surveys Tuts.*, vol. 13, no. 3, pp. 503520, 2011.

[5] Z. Ding, Z. Yang, P. Fan, and H. V. Poor, On the performance of non-orthogonal multiple access in 5G systems with randomly deployed users. *IEEE Signal Process. Lett.*, vol. 21, no. 12, pp. 15011505, Dec. 2014.

[6] J.-B. Kim, and I.-H. Lee, Capacity analysis of cooperative relaying systems using non-orthogonal multiple access, *IEEE Commun. Lett.*, vol. 19, no. 11, pp. 19491952, Nov. 2015.

[7] M. F. Hanif, Z. Ding, T. Ratnarajah, and G. K. Karagiannidis, A minorization-maximization method for optimizing sum rate in non-orthogonal multiple access systems, *IEEE Trans. Signal Process.*, vol. 64, no. 1, pp. 7688, Jan. 2016.

[8] M. F. Kader, S. Y. Shin and V. C. M. Leung, Full-duplex Non-Orthogonal Multiple Access in Cooperative Relay Sharing for 5G Systems, *IEEE Transactions on Vehicular Technology*, Vol. PP, No. 99, 2018.

[9] Y. Liu, G. Pan, H. Zhang, and M. Song, On the capacity comparison between MIMO-NOMA and MIMO-OMA, *IEEE Access*, vol. 4, pp. 21232129, 2016.

[10] Y. Dhungana and C. Tellambura, Outage probability of underlay cognitive relay networks with spatially random nodes, In Proc. *GLOBECOM*, Dec. 2014, pp. 35973602.

[11] Z. Ding, P. Fan, and H. V. Poor, Impact of user pairing on 5G non-orthogonal multiple access, *IEEE Trans. Veh. Technol.*, vol. 65, no. 8, pp. 60106023, Aug. 2016.

[12] Xuan-Xinh Nguyen, Dinh-Thuan Do, "Maximum Harvested Energy Policy in Full-Duplex Relaying Networks with SWIPT", *International Journal of Communication Systems (Wiley)*, Vol. 30, No. 17, 2017.

[13] Thanh-Luan Nguyen, Dinh-Thuan Do, "A new look at AF two-way relaying networks: energy harvesting architecture and impact of co-channel interference", *Annals of Telecommunications*, Vol. 72, No. 11, pp. 669-678, 2017.

[14] Dinh-Thuan Do, H-S Nguyen, "A Tractable Approach to Analyze the Energy-Aware Two-way Relaying Networks in Presence of Co-channel Interference", *EURASIP Journal on Wireless Communications and Networking*, 2016:271.